Results in Engineering 12 (2021) 100301

Contents lists available at ScienceDirect

Results in Engineering

journal homepage: www.sciencedirect.com/journal/results-in-engineering

Design improvement of a laboratory prototype for efficiency evaluation of solar thermal water heating system using phase change material (PCMs)

Greg Wheatley [a,*], Robiul Islam Rubel [b]

[a] College of Science & Engineering, James Cook University, James Cook Dr, Douglas, QLD, 4814, Australia
[b] Department of Agriculture and Biosystem Engineering, South Dakota State University, Brookings, SD, 57006, USA

ARTICLE INFO

Keywords:
Solar collector
Solar thermal energy storage
Solar thermal water heating system
PCM test Laboratory prototype
PCM blends
PCM efficiency Evaluation

ABSTRACT

Thermal energy in the solar thermal energy storage system cannot be stored for a long time during the evening hours as well as days that have minimal sunlight due to heat transfer to the surrounding atmosphere. PCMs are being implemented into these storage systems to enhance the thermal storage capacity of solar energy. PCMs based latent heat storage technique can extend thermal energy storage over long periods due to its ability to store energy. Several different types of PCMs with various chemical compounds and melting temperatures can suit various thermal storage applications in real life. However, the concept of combining these PCMs types with different ratios is an area within this field that has not yet been investigated as it is time-consuming and a matter of numerous combinations and trials. A model solar thermal energy storage system with the flexibility to test different PCM's blends can omit the problem. This research work intended to propose a design as testing apparatus that can successfully operate and investigate the different PCM's blends to find the optimum ratios for a highly efficient solar thermal water heating system. An appropriate laboratory-sized prototype design has described that can replicate the functions of a solar thermal water heating system. The necessary assumptions and mathematical relations are also presented for the proposed design.

1. Introduction

The increasing use of energy by the huge population of the world has put an immense amount of pressure on the demand for easily accessible energy [1,2]. Fossil fuel energy sources are running extremely low due to being consumed enormously by the rapidly swelling population [1–7]. With this depletion in fossil fuel energy, the world also faces the increased influence in different types of pollutants like greenhouse gases, toxic materials, etc. on earth [3–6]. These important factors have a large amount of research turn towards developing and using renewable energy sources such as solar energy, wind energy, and hydropower [6,8–11]. Solar energy is one of the most lavishly used renewable energy sources in Australia used to combat the energy crisis with minimal environmental impact [7,10–13]. Compared to other continents, Australia has the highest solar radiation per square meter, due to its deserts in the northwest and the center of the continent [12]. Australia receives on average 58 million PJ (Petajoule) per year [14]. Annually, some areas of the continent are posed averagely to 10 h of sunshine per day providing a great window of using solar energy for this continent (Fig. 1) [14].

According to the Australian Renewable Energy Agency, 21% of Australian households now have rooftop solar panels to store solar energy in various forms [15]. However, the biggest drawback to this energy source is the storage of energy generated from solar radiation during sunshine hours [7,9,16]. Since solar energy cannot be stored fully for lack of storage devices and be used after daytime, the solar appliance becomes insignificant to the consumers as the energy generated by sunlight slowly degrades to 0% [7,16,17]. To overcome this scenario, the concept of a solar thermal energy storage system needs to be industrialized broadly [7].

To be noted that, solar energy is classified into two different types of mechanics; Solar Thermal Energy which is defined as the alteration of solar radiation into heat energy, and Solar Photovoltaic (PV) where using photovoltaic cells can directly transform the sunlight into electricity [6,17,18]. The solar thermal energy storage system can be divided into further types such as sensible heat storage and latent heat storage, with more preference towards latent heat storage due to its higher heat storage capacity and isothermal behaviour during charging and discharging [2,7,16,19]. Alike a normal thermal energy storage system, to captivate solar thermal energy storage system works on the

* Corresponding author.
E-mail addresses: greg.wheatley@jcu.edu.au (G. Wheatley), rubel.ruet10@gmail.com (R.I. Rubel).

https://doi.org/10.1016/j.rineng.2021.100301
Received 26 July 2021; Received in revised form 2 September 2021; Accepted 17 October 2021
Available online 18 November 2021

same principle except the source of energy is solar heat.

For example. Solar pond, a mechanism to heat water for generating electricity using low boiling temperature fluid is on research in recent years to store solar energy. Ranjan Das et al. [9–11,20–22] working on a thermoelectric energy generation system using a solar pond where they are using solar energy for storing heat in the water to generate electricity. Solar pond work as a bulk heat storage system here. On small scale, the storage method may be some other way like using chemicals, blends of chemicals or metals, etc. to heating water in need. Therefore, it's clear to use some medium as mandatory to store solar thermal energy. Though a lot of progress has made, modern times still lacks behind to capture and store all the solar energy incidents in a particular area of concentration. Moreover, the solar thermal energy storage system is less popular around the world due to its storage problem and few research centres working on their development to increase the efficiency of the storage so far.

On the ground of storing thermal energy, PCMs regards as the best categories of materials to serve versatile purposes and various temperature ranges. So can be for solar thermal storage systems [2,23]. PCMs are considered heat storage materials as they have been used widely to boost the energy storage volume of various thermal energy storage systems [2,24,25]. The performance of the solar thermal storage system largely depends on the PCMs used for the system [2,24,26,27]. It plays a crucial role in energy storage as the temperature of the source increases. PCMs go through chemical breaking within which leads to the phase transition most commonly solid to liquid as they absorb additional energy coming into the system [19,24,27]. The stored energy in the PCMs can later be released into the pre-designed system.

PCM based thermal storage devices are being used in solar power generation, solar cookers, solar dryers, etc. [27]. Another common use for PCMs based solar storage systems is heating the water for the buildings required for most snow areas of the world, especially remote areas [26,27]. The hot water is needed for occupants of the cold area, processing industries can be supplied from solar thermal water heating system easily in a relatively inexpensive manner. The solar thermal water heating system generally does not consist of any complicated equipment providing the benefit of easy fabrication and low maintenance.

However, this field is comparatively new, and few researchers have found using an appropriate design of PCMs based solar thermal water heater system. The objective of this research is to investigate and develop a design analysis that will be suitable to replicate a typical solar thermal water heating system. This storage system will be able to test various PCM types and combinations to understand their influence in storing thermal energy.

This work also specifies and discusses all design decisions, drawings, manufacturing strategies, and technical specifications needed. So, a successful testing facility can be proposed by discussing the usage of PCMs as a thermal energy storage unit and its various classifications to discover what combination of PCMs work most ideally in the solar thermal water heater system. Also confers to what storage system works better and can be used accurately with real-life limitations. To achieve this goal, the researches also reviews the literature surrounding this topic including similar testing facilities to base this design from as well as key design considerations to ensure testing success. Then using relevant Engineering Technical Specifications and Design Analysis Techniques a final design has suggested.

2. Motivation

PCMs are a revolutionary product in the field of renewable energy sources as these materials can absorb the energy during the day when the source is present and then release the energy as required after dark thus making solar energy viable during no sunshine [27]. The use of PCMs in latent heat storage systems has been under the radar of researchers for a very long time but very recently this method of energy

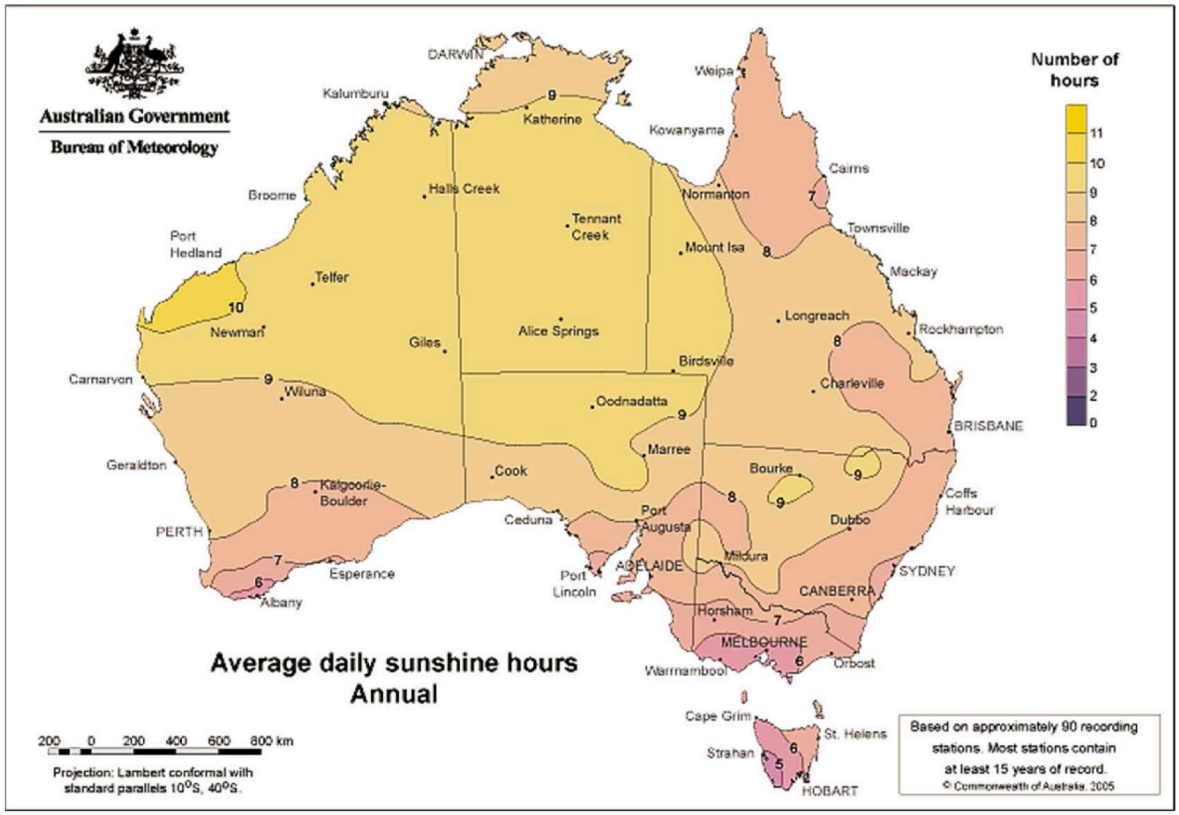

Fig. 1. Average daily sunshine hours annual.

utilization has received much attention from the energy sector [27]. Even though energy provided by these systems is at a higher cost than fossil fuels, their restricted influence on the environment of the earth and ozone layer and the sustainability of the energy resource is the major advantages over the fossil fuels that cannot be easily ignored by the energy sectors [19,25]. Solar thermal energy storage system design is an important factor when constructing the solar thermal water heating system [27]. Researchers have openly discussed the design limitations but still, many researchers stand divided upon what the ideal shape of the solar thermal water heating systems should be.

In the literature review, it has been found that one PCM can be combined with a different class of PCMs to develop a more ideal PCM that can have a very strong thermal conductivity [28]. The most useful device industrialized to harvest this benefit is the solar thermal water heating system. This system comprises of PCMs which act as a key component to utilize the heat from the source and store the energy. It has been established that the unsurpassed PCMs to be used in solar thermal water heating systems are fatty acid combinations and the second most commonly used PCM is paraffin wax [27,29]. The reason that they hold a higher rank than the other PCMs is that these two PCMs have good chemical stability, nontoxicity and melting points are suitable for solar heating applications [27,29].

There are a lot of researchers working on the PCM in the experimental tests. Most of them concentrated on working and testing on their chosen PCM. For example, G. Murali et al. [30], M. A. Fazilati et al. [31] worked for testing PCM. They used a fixed system to test and did not mention that wither their method is appropriate for testing any PCM or just a specific one. Jacobo Porteiro et al. [32] presented a facility and method to study the thermal effect of multiple PCMs. But the equipment and facility are much more complex and costly to study a wide variety of PCM for the solar thermal heating system. Good evidence of the lack of having any unified simple system to test different PCMs for solar water heating system can be presented referring the review article of Eleni Douvi et al. [33] published in 2021. This article has listed the research on solar domestic water heating, where most of the research is either experimental or experimental with simple mathematical analysis. 90% of cases highlighted in this review have a single PCM test experimental approach. The reason behind the situation lies in the lack of a small laboratory scale prototype that can be used for the multiple numbers of PCM blends. Since solar thermal water heating systems are still being debated regarding which design and PCM blends are better to make the most of solar energy, a configuration must be invented to test different PCM blends at a low cost.

3. Designing improvement of a PCM based solar thermal water heating system

Typical solar water heating systems usually involve of flat plate collector attached to a thermal energy storage system [9,34]. In this particular system, the PCMs are filled within the copper tubes and placed vertically. The length of these PCM tubes is selected as only a few inches shorter than the height of the cylinder [34]. This design is considered very simple and the PCM materials used are paraffin wax and stearic acid thus making this system inexpensive as paraffin and stearic PCMs are very commonly obtainable [35,36]. According to Sharma et al. [35], a salt hydrate-based integrated collector can be set up for providing hot water. Demonstrations were done to prove that the thermal efficiencies of such systems can be enhanced by combining multiple different class PCMs which can be used as latent heat storage devices.

Since PCMs naturally have low thermal efficiencies, the salt hydrates were encapsulated in a special corrugated-fin heat exchanger. The limitations faced by these storage systems were multiple as encapsulating the salt hydrates increased the thermal conductivity, but the cost of this thermal energy storage also skyrocketed. Another constraint that was faced by this design was the leakage of salt hydrates from encapsulated form to the liquid thus causing problems in manufacturing this unit. Overall flat plate PCM-based solar water heater storage system is considered more because of its simple design, which is easier to manufacture, and it is less costly than others.

For this investigation it is preferred to use latent heat storage over sensible heat storage as this specific storage has multiple advantages for example: with only a small temperature differential it can stock a massive quantity of heat energy [2,19,37]. Another advantage is the storage densities can be reached from 5 to 10 times higher for multiple PCMs [2,19,37]. Latent heat cannot be solely stored on its own, the PCM must endure an increase in its internal temperature in order to reach the process of phase transition point which is also represented by the storage of sensible heat [7,38].

Also, the amount of heat storage depends on the specific heat capacity of the storing medium, the temperature change before and after storing, and the total amount of storage material. If we consider a melting solidification phase change for a PCM material, then the latent heat storage capacity can be characterized by the following equation (1) that integrated as equation (2) [7,39] -

$$Q = \int_{T_i}^{T_m} mC_{sp}dT + ma_m\Delta h_m + \int_{T_m}^{T_f} mC_{lp}dT \tag{1}$$

$$Q = m\left[C_{sp}(T_m - T_i) + a_m\Delta h_m + C_{lp}\left(T_f - T_m\right)\right] \tag{2}$$

The sensible heat stored by the increase in the temperature of the material from its initial conditions to the phase change temperature is denoted by the first term in the equation, the next term represents the latent heat of the material during the phase change energy storing, the quantity of material also impacts the heat energy stored by the PCMs [38]. Since Q (Eqs. (1) and (2)) depends on the storing material's specific heat capacity, PCM with high specific heat will be beneficial for design [40]. These mathematical relations also indicate finding a good PCM or mixture of different PCMs for any purpose.

To be stated that, designing and modeling the solar thermal water heater system will help to achieve the optimization of manufacturing the unit for the solar collector characteristics, comparison between PCMs, and many other essential approximations such as solar panel collector size, improving efficiency by perfecting the tilt angle and estimating the cost-effectiveness of solar thermal water heater system when compared to electricity [41]. The basic model (Eq. (1) & Eq. (2)) has numerous sub-components to be taken care of for a real-life solar thermal water heating system. The solar thermal water heating system in this research is also built of multiple different parts such as solar panels (collectors), storage tanks, heat transfer fluid, and most importantly PCMs [41,42].

3.1. Designing for solar collector efficiency

The selection of solar collector depends upon the temperature production essential by the system as unglazed collectors are mostly used for low-temperature applications [43] while glazed or flat plate collectors [44] are the first choice of researchers for solar water heater storage systems as they possess high insulation thus heat loss will be less [41,45]. Common glass is mostly used as transparent cover material in solar collectors even though it possesses all the required properties. It is rather heavy and brittle with thickness from 3 mm to 4 mm, the only issue being it has low solar transmittance [46]. There is however an alternative present called tempered glass, this glass is already being used in many collectors for its advantages like higher collector efficiency, safety, and mechanical strength also this glass has higher transmittance towards solar energy in comparison to common glass [46]. The design of the hot water storage tank is made while keeping the pressure constraints in mind with another significant design limitation being corrosion protection. The most common material used for designing the storage tank is mild steel for reasons like strength possession for pressure requirements and wall thickness of 2–3 mm corrosion protection on the

inner side of the water tank can be achieved by coatings of glass enameling or galvanizing [46].

To design the model (Figs. 2 and 3) with utmost accuracy in predicting the solar collector efficiency [47] we have considered using flat plate collectors and will also develop an equation to analyze the effect of solar collector efficiency on the volumetric flow [41], the equations are presented below. The radiant flux striking the plate collector (R_f)-

$$R_f = T_{cov} A_p G \tag{3}$$

Since only a fraction, $\propto_p$ is absorbed and plate being warmer than the surrounding loses heat at a rate of $(T_p - T_a) / R_1$. The heat remaining in the collector after loses is terms as input energy in this case. Using the Hottel-Whiller equation as presented in Ref. [41] we obtain the following relationship-

$$P_u = T_{cov} A_p G - \left[(T_p - T_a) / R_1\right] = \exists_c A_p G \tag{4}$$

In equation (4), $\exists_c$ is always $\exists_c < 1$ as no ideal system can hold all the incident rays. The temperature difference between the plate and fluid should be small and $\exists_c$ also should be slightly less than 1 for a well-made solar collector [41]. Afterward, the solar thermal efficiency of the collector can be estimated by the straightforward relation of the heat given to the water of the system to the amount of heat the solar collector is receiving-

$$\eta_c = \dot{m} C \Delta T / A_p I \tag{5}$$

where the mass flow rate is

$$\dot{m} = \eta_c A_p I / C \Delta T \tag{6}$$

where $\Delta T = T_2 - T_1$. Using equations (4)–(6), the collector efficiency can be determined and later used for determining the overall efficiency of the solar water heating system.

3.2. Design analysis and modification of keys parts

The following part of the article will present the detailed engineering analysis completed to develop the final design to meet the requirements of the research question proposed. The research questions and requirements of initial designs are already found in the literature for similar applications, focusing particularly on the key components that would influence and hinder the final design to be developed. Necessary heat transfer principles and equations backed with several calculation processes were also used to validate the performance and overall dimensions of a PCM-based solar thermal water heating system testing apparatus. These calculations assist to understand how the water, PCM, and overall apparatus are behaving in the changing temperature environments. The structural members of this apparatus were analyzed using Finite Element Analysis (FEA) based on the Computer-Aided Drawn (CAD) models of the final design. Through this analysis, a validated and accurate final design will be developed that will meet the specifications of testing different PCMs in a solar thermal water heating system testing apparatus.

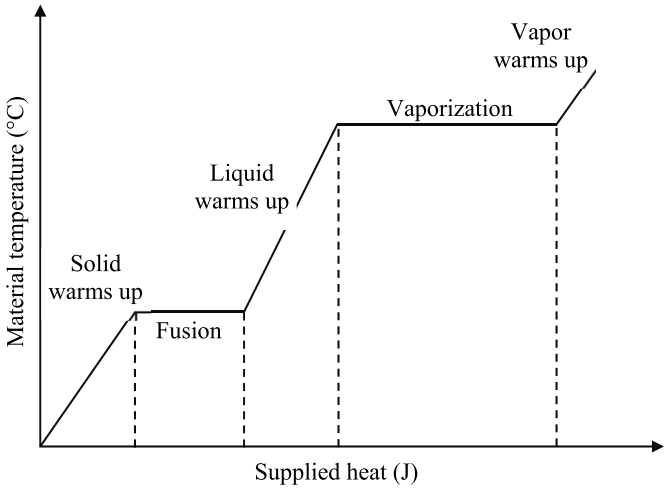

Fig. 2. PCM temperature profile in relation to heat supplied.

3.2.1. PCM storage design

The *first* storage tank design that was identified and analyzed for this investigation was from a study completed by Kumar and Mylsamy [48] that uses a tube arranged solar water heater accompanied by a storage tank where different PCMs can be tested. This solar heating apparatus is used for PCM testing purposes as the water storage tank has an in-built container where different PCM materials can be applied to absorb the thermal energy from the solar heater. A detailed schematic of this apparatus, as well as the PCM container within the storage tank, can be seen in Reference [48]. This water heating apparatus relies on thermo symphonic flow to allow water to travel through within the pipes transferring ambient temperature water to hot water and into the storage tank [48]. The storage tank which has a capacity of 100 L made of stainless steel has a smaller PCM container made of aluminum which stored paraffin wax and Silicon Dioxide Nanoparticles (SiO_2, Silica) at approximately 15 nm in grain size [48]. The horizontal storage tank also has 5 cm thick polyurethane foam for insulation with all joins and openings airtight to increase thermal efficiency, the glass pipes are held within the optimum tilt angle range (10°–15°) to receive maximum radiation from the sun [48].

The main advantage to this design was the ability to test PCM variables in direct sunlight allowing 24–48 h individual tests to be completed. Using the specifications based on the literature article a CAD model of this design was developed to investigate the structural loading on the frame due from the water tank and the evacuated tubes. This static structural FEA analysis was completed using ANSYS Workbench 19.2, and the Equivalent Stress and Total Deformation outputs can be observed in Fig. 4(a–b). From observing the FEA outputs it is evident that this design is over-engineered as the maximum equivalent stress is very small 4 MPa. The PCM storage tank in the center of the water tank is a poor design choice as the interaction between water and PCM is restricted to a confined area within the tank, this will minimize thermal efficiency. This testing apparatus design is mainly suitable for testing conditions that occur over long periods. For our research investigation, we would prefer to design PCMs test in shorter time frames. This is due to the limitless possibilities of combinations with varying ratios to test, it would be more suitable to test using a heating element to heat the water to the desired temperature accurately and then record the cooling profiles. This is also validated as it would be expensive to purchase solar evacuated tubes as well as have them fitted properly due to their brittle nature.

The *second* design which was developed by Sharma et al. [35] encompasses a steel cylindrical drum with several tubes within, designed to hold and segregate the PCM from the Heat Transfer Fluid (HTF). This design did not have any images to reference the design, however, the key dimensions found with relation to the schematic provided were identified in Fig. 5. When this design was drawn in Solidworks it was observed that there was no support securing the cylindrical tubes vertically making the process of FEA impossible to get reliable results. It was decided to input support towards the top of the drum to keep the tubes straight. The model can be seen in Fig. 5. It was calculated based on the volume of the storage cylinder subtracting the volume of all tubes from the maximum amount of water that could be applied without overfilling the system is 250 L which converted to force is 2.4 kN. Alongside this force, 30 kg of PCM mass was applied to this design, whilst creating fixed support underneath the storage cylinder, the FEA simulation output screenshots can be seen in Fig. 6(a–b). It can be observed that the maximum stress is occurring at the bottom of the cylinder which is

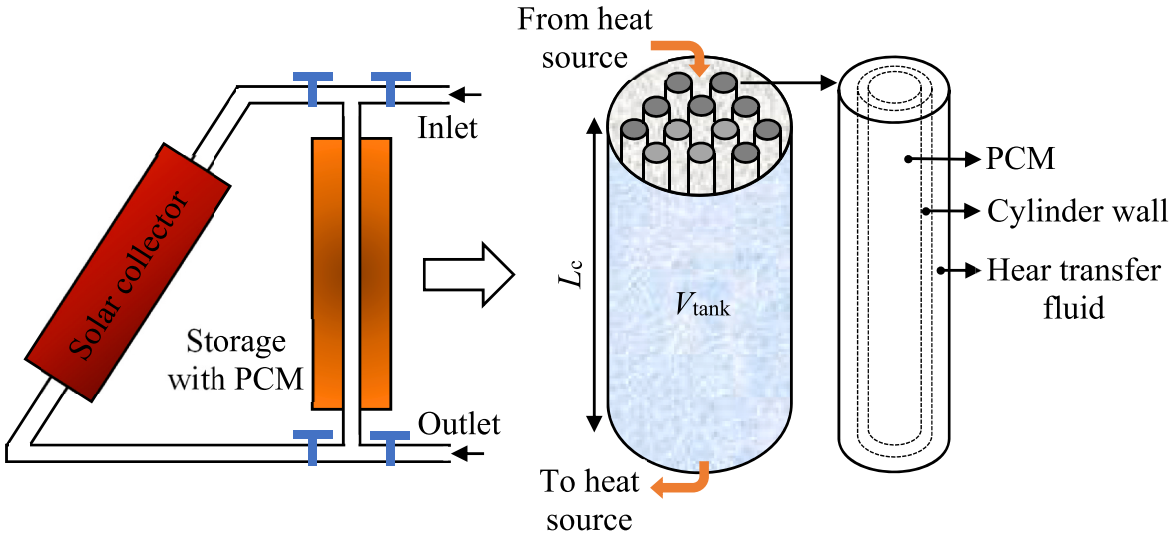

Fig. 3. A schematic of a solar collector.

expected as this is where the load is positioned in the system. It was recorded that only 0.5 MPa of maximum stress is occurring at the bottom of the cylinder, this small amount proves this design can easily handle the water and PCM weight in the system.

The use of PCM tubes is a simple but useful technique to gain adequate interaction between the PCM and the water itself. The use of a simple cylindrical tank would be lightweight when empty and easy to manufacture. The ability to tip the water out after each use is simple but would be effective. This would also be the case for the PCM tubes as simply pulling them out after use for cleaning and replacing the PCM type is simple and effective for this testing environment. Due to this design only holding the water and tubes, the amount of force applied would be negligible. The only parameter that would not be used is the support for the tubes. Using a frame that could also harness the heating element would be useful for the final design. Overall, these initial designs have identified the critical design decisions that need to be made for the final solution, using these designs as a reference has identified areas to be investigated further as well as areas that should be avoided. These designs are useful for PCM testing but to the best answer, the research question proposed earlier, a new design is required.

3.2.2. *Water tank design development*

The final design that has been chosen encompass a water tank to store the water similar to that developed by Sharma et al. [35] where a cylindrical tank was used that hold several PCM tubes. It has been found in the literature that there are calculations that can be made to design the water tank optimally, the main calculation that will be completed can understand the volume of the tank based on the intended height and the number and dimensions of the PCM tubes that will be used. This formula from Li et al. [49] can be observed by-

$$V = n\pi D_{out}^2 l \,/\, 4(1 - \varepsilon) \tag{7}$$

For the final design, the length of the cylinder has selected as 400 mm and the water fraction has assumed as 80%. The number of PCM tubes considered for the design is six. This was chosen as it is intended that a large amount of PCM can be tested during the large-scale tests. It is also intended that a heating element can also fit inside the tank for heating purposes so for this investigation six PCM tubes will be suitable. The PCM tubes under consideration are an off-the-shelf aluminum tube that can be cut to any length withinner diameter of 50 mm and a thickness of 1.6 mm (D_{out} = 53.2 mm). Substituting the values, the volume of the tank required for testing can be found as $V_{tank} = 0.0266$ m^3 or 26.6 L. Using this volume value, the ideal radius (r_{tank}) and followed by the diameter ($D_{tank} = 2r_{tank}$) for the tank can be calculated which are 145 mm and 290 mm respectively. For this design, the height of the tank (l) was adjusted to 450 mm after this calculation process to stop overfilling. For testing, this height line should be used as a marker to know how much water is required for successful testing. The amount of water required ($V_{water} = V_{tank}$ - V_{tube}) for testing can also be determined using these values, as it is simply subtracting the volume of the tubes ($V_{tube} = \pi r_{tube}^2 l$) from the volume of the tank ($V_{tank} = 0.0266$ m^3). Using $r_{tube} = D_{out}/2$, the $V_{water} = 0.0172$ m^3 or 17.2 L.

With the key dimensions of the tank identified, this new tank was then modeled using the Solidworks 2019. This tank and the water within can be considered the baseline in terms of thermal efficiency, as the time taken to cool the water with the influence of PCM can be compared to the time without PCM for analysis. Essentially, it would be expected that the time to cool the tank with the influence of PCMs inside the aluminum tube would be significantly longer than without PCMs. Unfortunately, these states cannot be modeled using Computational Fluid Dynamics (CFD) due to the issues with floating point error as ANSYS cannot recognize the phase change in a material. Fortunately, though using the natural convection process, several key heat transfer parameters can be developed to understand the baseline time to cool the tank without PCM influence [50]. This involved calculating the heat transfer coefficient 'h' (W/m°C).

The first parameter needed is the maximum temperature that is tested was found in the literature that Paraffin Wax with the best thermal properties has a melting temperature of 75°C. So, for this investigation, a maximum temperature of 80°C was used (any higher water boiling would occur). The film temperature (T_f) required (equation (8)) to calculate thermal properties can be observed below, the minimum (room) temperature that used is 20°C.

$$T_f = (T_{max} + T_{min}) \,/\, 2 \tag{8}$$

At 50°C the key properties for air were consulted from thermodynamic tables. Using this value called Rayleigh's number (Ra) which is the relationship between buoyancy and viscosity for the surrounding air to the tank can be found by-

$$Ra = \left[g\beta\,(T - T_\infty)l^3\right] Pr \,/\, \nu^2 \tag{9}$$

where $\beta = 1/T_f = 0.00309k^{-1}$. For natural convection calculations, the tank can be considered a vertical plate for calculation if the diameter of the tank is greater than the following formula-

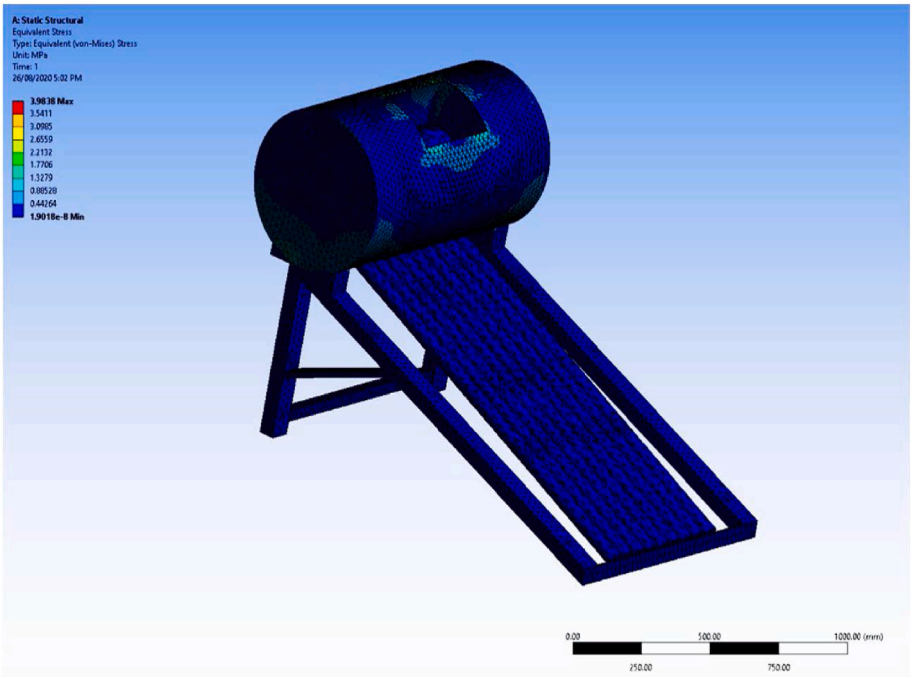

(a): Initial design 1 equivalent stress response

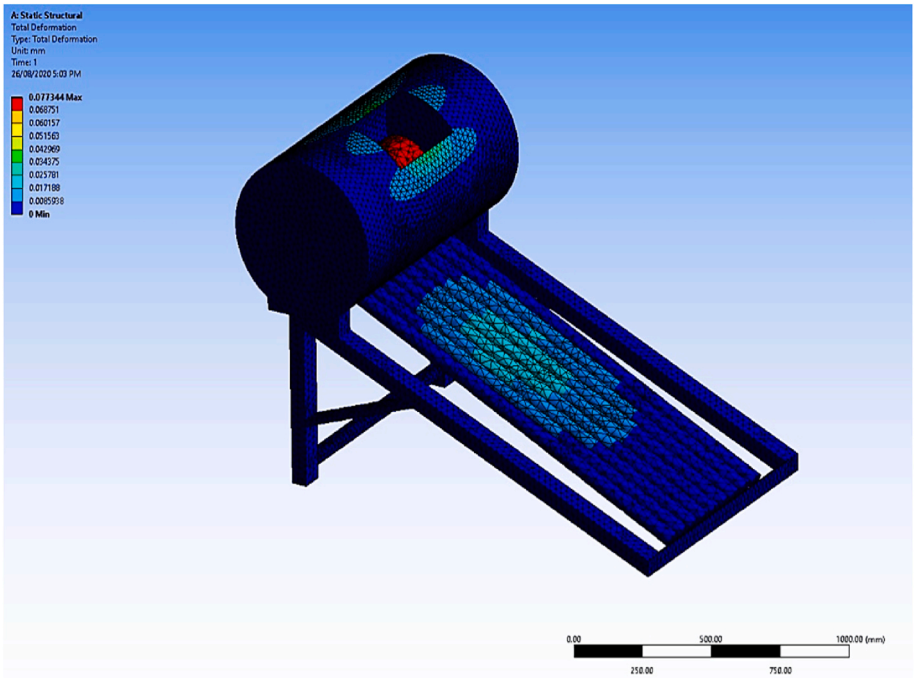

(b): Initial design 1 total deformation response

Fig. 4. (a): Initial design 1 equivalent stress response. (b): Initial design 1 total deformation response.

$$D_{Tank} \geq \frac{35l}{Gr^{0.25}} \tag{10}$$

where $Gr = Ra/Pr$. Using the relevant value in the above equations is $D_{Tank} = 0.290\,m \geq 0.101\,m$. This proved the vertical plate assumption can be followed. Due to the Ra ranging between 10^4–10^9 the Nusselt number formula $Nu = 0.59 \times Ra^{0.25}$ can be followed. Finally, the desired heat transfer coefficient (h) can be developed using the following relations $h = (Nu \times k) / l$. This heat transfer coefficient $h = 5.123\,W/m\Delta^{\circ}C$ helped to determine the time it will take to cool the water. Assuming the tank is a Lumped System meaning the temperature is spatially uniform the time (t) taken to cool the tank can be found using

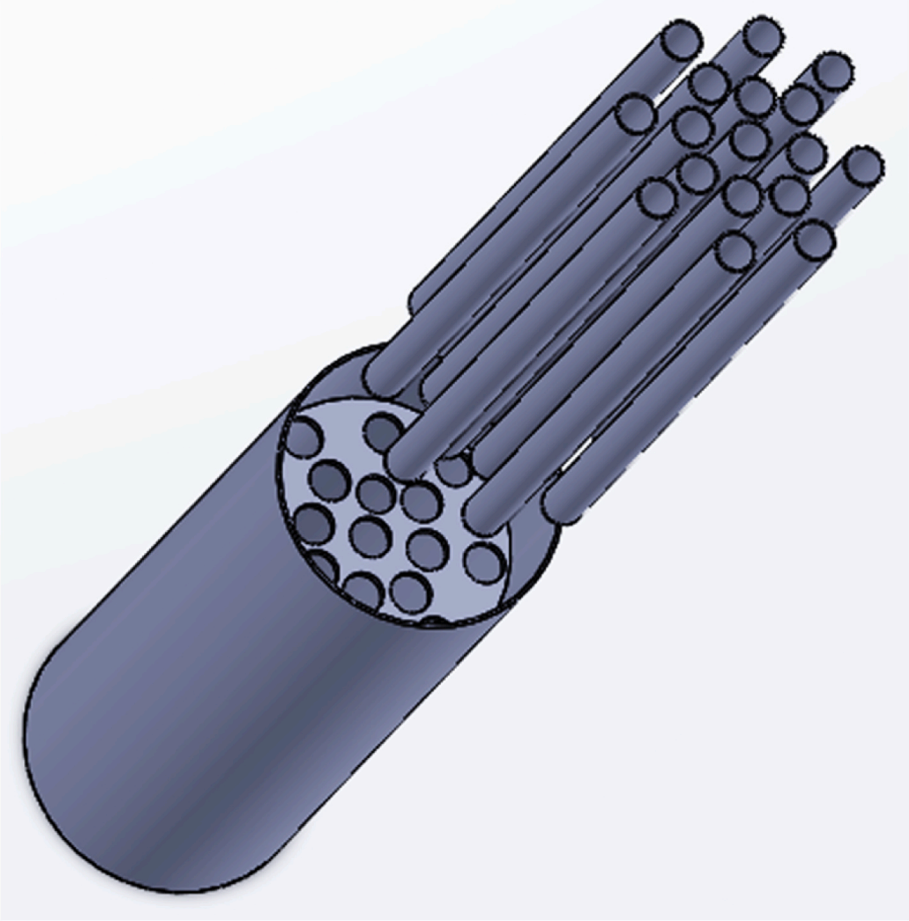

Fig. 5. Initial design 2 exploded view.

the following formula-

$$t = (\rho C_P \ / \ h)(V \ / \ A)\, ln[(T_\infty - T_0) \ / \ (T_\infty - T)] \quad (11)$$

where the ρ and for water at room temperature is 998 m^3/kg and 4.2 J/kgK respectively, and the relative value $V/A = \pi r^2 l / \pi r^2 = l = 0.4$. Plotting this formula and the relative values into Microsoft Excel and letting the value 'T' interchange in one-degree intervals a plot describing the cooling profile over time can be developed (Fig. 7). It can be noted how it described an exponential profile. Viewing Fig. 7, the time taken to reach 25°C is 951.95 s, or equates $t = 15.86$ min. Using this time as the baseline the analysis can be completed through testing PCMs to see the effect in time increase. It was decided for this design component that Static Structural FEA would not be completed due to the design being similar to that by Sharma et al. [35] as 250 L of water and 30 kg of PCM were used. It was found from this FEA that minimal effect was developed in terms of stress and deformation, so for this final design, it can be neglected.

3.2.3. PCM tubes and fin design

The next component required for the final design is the tubes to hold the PCM. For the simplicity of this component, it was decided to purchase these tubes off-the-shelf as it is a cylindrical aluminum tube with a cap on the end (Fig. 8). aluminum was selected as the desired material due to its low cost, lightweight, high melting temperature, and its ability not to corrode from the PCM. The cap on the end is also an off-the-shelf aluminum part that securely fits over the end of the tube ensuring no PCM escapes. It was identified previously in the tank volume calculations that the inner diameter of the tube is 50 mm and has a thickness of 1.6 mm. For this design, a lot of effort has been given considering other areas in which the thermal performance of PCMs and the heated water could be enhanced. It was identified that implementing extended surfaces or Fins to the PCM tubes may have an effect in prolonging the heat in the system. Due to the cylindrical design of the tubes, it was decided that using eight annular fins would be implemented to the pre-existing tube structure by a stick welding process. An image of a CAD modeled PCM Tube with annular fins can be observed (Fig. 9).

The key dimensions of these fins are based on calculations made to have a high fin efficiency (η_{fin}), as with a high η_{fin}, the amount of heat transferred from the PCMs to the water can be high. The key parameters as well as the plot to calculate η_{fin} can be observed in the standard fin efficiency curves with a schematic detailing the heat transfer process of fins (Fig. 10). Using standard fin efficiency curves, η_{fin} could be determined. For thermal conductivity (k) of aluminium at the $T_f = 50°C$ is 0.5 W/m.K and fins were set at Length (L) = 10 mm, thickness (t_h) = 10 mm, and based on the dimensions of the tube specified previously radius $r_1 = 26.6$ mm. The horizontal quantity of the standard chart can be found by Ref. [51]-

$$\xi = L_c^{3/2}\left(h \ / \ kA_p\right)^{0.5} \quad (12)$$

where $L_C = L + t/2$ and $A_p = L_C \times t$. Consulting Line 1 on standard η_{fin} curves, using this horizontal axis value (ξ) the η_{fin} was estimated as 87%. To understand the influence of annular fined PCM tubes heat transfer (Q_{fin}) to the water, it is important to understand the baseline heat transfer of the tubes without the fins. The calculation process to find the Q for a singular tube and the total six tubes can be observed by-

$$Q_{Total,\ no\ fins} = h_{no\ fins} A_{no\ fins}(T_2 - T_1) \quad (13)$$

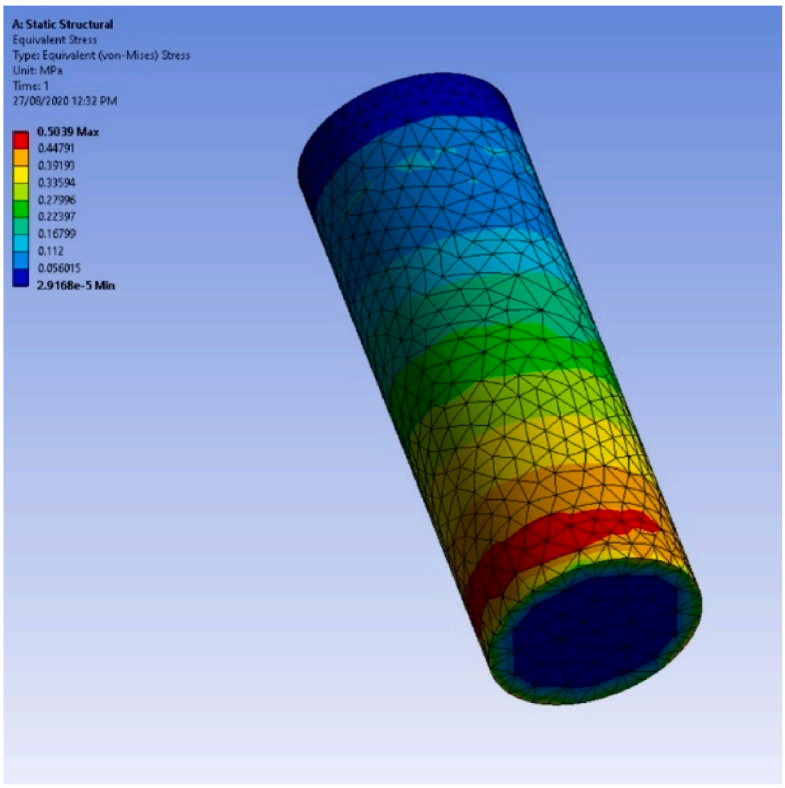

(a): Initial design 2 equivalent stress response

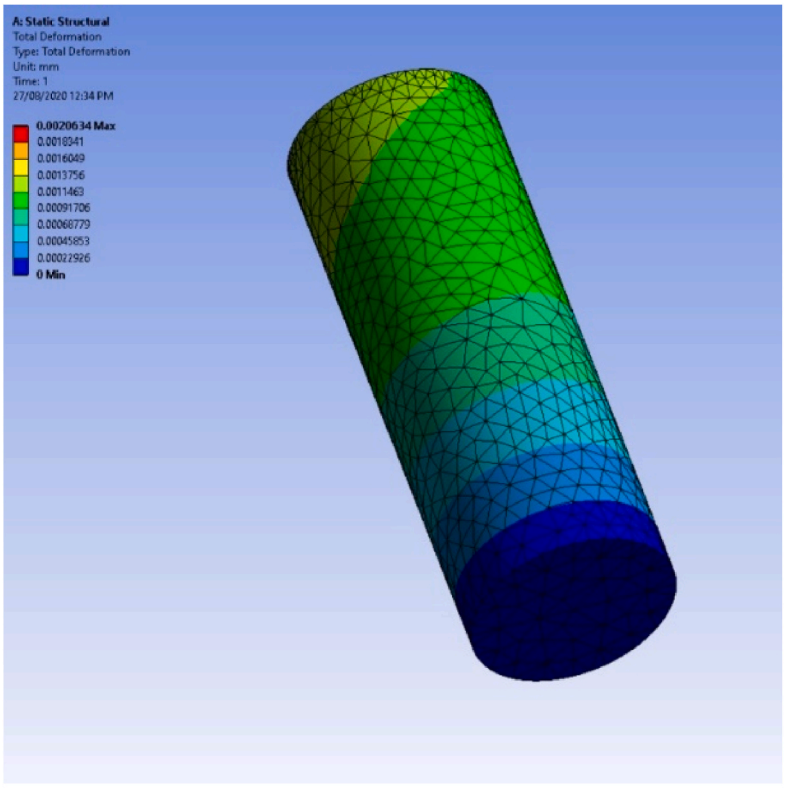

(b): Initial design 2 total deformation response

Fig. 6. (a): Initial design 2 equivalent stress response. (b): Initial design 2 total deformation response.

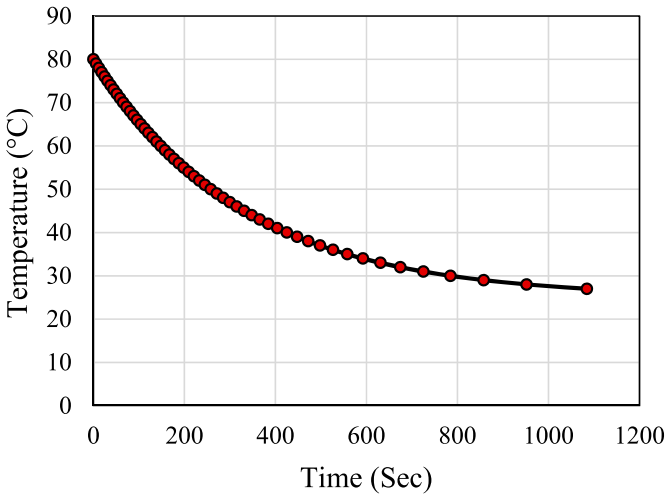

Fig. 7. Water tank Lumped capacitance cooling profile.

Fig. 8. Aluminium tube (left) and end cap (right).

where $A = 0.0653\,m^2$. With this value, the heat transfer for single tubes with no fins ($Q_{Single\ tube,\ no\ fins}$) is 18.4 W. Therefore, for six tubes the total heat transfer ($Q_{Total,\ no\ fins} = Q_{Single\ tube,\ no\ fins} \times 6$) becomes 110.4 W. Using the η_{fin} developed earlier, the heat transfer with respect to the influence of annular fins can be observed by-

$$Q_{finned} = \eta_{fin} h_{finned} A_{finned} (T_2 - T_1) \tag{14}$$

where $A_{finned} = 0.0833\,m^2$. With this value, the heat transfer for single tubes with fins ($Q_{Single\ tube,\ finned}$) is 20.42 W. Therefore, for six tubes the total heat transfer ($Q_{Total,\ finned} = Q_{Single\ tube,\ finned} \times 6$) becomes 122.52 W.

This shows for the overall system that there is a 9.9% increase of Q when the PCM tubes are implemented with extended surfaces. However, this is just the baseline without the influence of PCMs so it will be expected that the influence of PCMs will significantly improve the overall thermal performance. Due to the PCM tubes only holding PCM and the weight of these being at the maximum 30 kg which is sat at ground level, it has been deemed that Static Structural FEA is unnecessary as the tubes will easily be able to hold the required amount of PCM weight.

3.2.4. Water heater development

In order to replicate the solar thermal temperatures experienced in an actual solar heating system, it has been decided that a heating element will be used. Due to the nature of this testing apparatus being short and quick, various PCM combinations and ratios can be tested and explored in a small time frame. This was also decided as the frame will not be insulated and will be open to the atmosphere reducing the time to cool meaning a reduced testing time. It was important to use a heating element that will be able to increase the temperature quickly and accurately to the desired level. Based on these key points, a SCINTEX Immersion Heater [52] was used. This heater has a built-in digital thermostat that can be mounted to increase testing accuracy. The heating element was a vertical probe that is 400 mm long which with it mounted to a frame an adequate amount of contact between the element and water will be created, thus improving heating time. The heater has a maximum temperature of $100°C$ and a power output of 2400 W which suits the parameters of testing [52].

3.2.5. Frame development

The last component of this final design is the frame that holds the heating element as well as positions the PCM tubes in the upright position. The frame is designed to sit over the top of the water tank with a hole in the middle for the heater to be supported from as well as allow the heating element to sit in the water tank, the heater fitting is 50.8 mm (2 inches), so the hole was designed to cater for this. Surrounding the heater hole in the six PCM tubes holes which are not used to hole the tubes only to give support, so they do not fall over spilling the PCM. Due to the water being stationary, it was decided that letting the tubes freely sit in their holes is the simplest and most effective method for testing. The frame is made from $30 \times 30\ mm^2$ SHS (Square Hollow Section) Steel and 1.6 mm thick galvanized steel which is leftover from the sheet used to develop the water tank. There is an amount on the side with the same 1.6 mm galvanized steel used to hold the digital thermostat for the water heater. Due to the mass of the heater being 5 kg (50 N) and the thermostat being 3 kg (30 N), Static Structural FEA was completed to analyze the loading. Based on the design and selection of appropriate material it is specified to weigh 15 kg which is lightweight and easily maneuverable by hand. The relevant Static Structural FEA for this frame can be observed in Fig. 11(a–b).

Observing the FEA output for Equivalent Stress and Deformation, it can be confidently said that this design will adequately meet the requirements of holding the immersion heater and thermostat control. With the frame being lightweight, it can easily be positioned by hand, it is also versatile as the PCM tubes can be removed and replaced without much effort. As there is no deformation occurring in the galvanized sheet metal covering the top region of the frame it is an excellent design decision to reuse the off-cuts from other components, thus saving money. It can be observed in Fig. 11(a) that the plate holding the thermostat will also adequately handle the small weight being fixed to the location.

3.2.6. Apparatus material specifications and compliance of design

To ensure this design is successful and will not succumb to failure, potentially injuring bystanders the design must comply with relevant Australian Standards. This section provides comprehensive evidence through appropriate technical specifications such as through Australian Standards to ensure this design is compliant and therefore successful for development. The materials used to manufacture the new PCM-based solar thermal water heating system testing apparatus are broken into the four main components that constitute this design.

Firstly, the water tank was selected as hot-dipped, Zinc coated with galvanized sheet metal. Consulting AS/NZS 2312.2–2014 [53] for hot-dipped galvanized steel it is important to prevent corrosion that could affect the performance of the tank. Post-welding water soluble

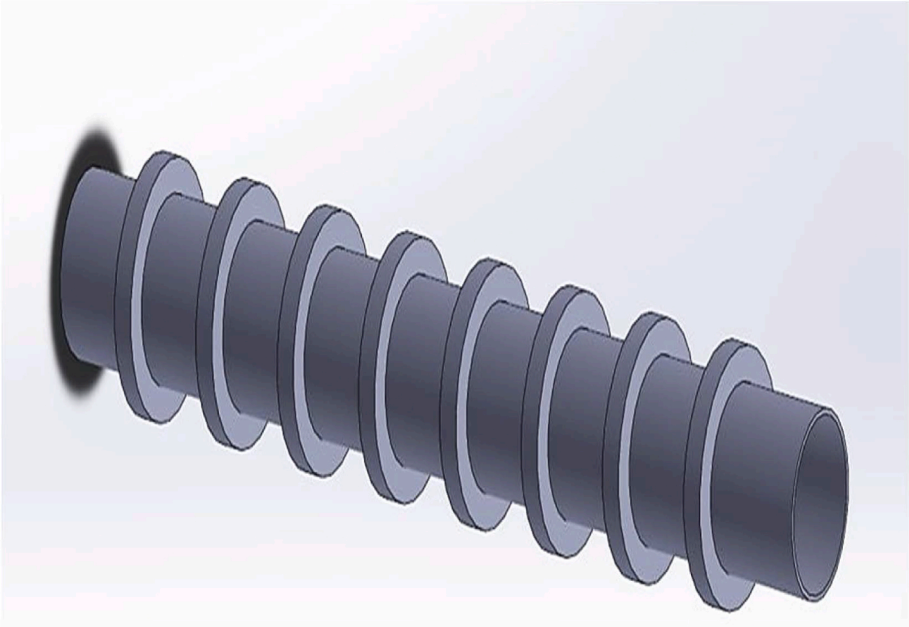

Fig. 9. CAD annular fin design.

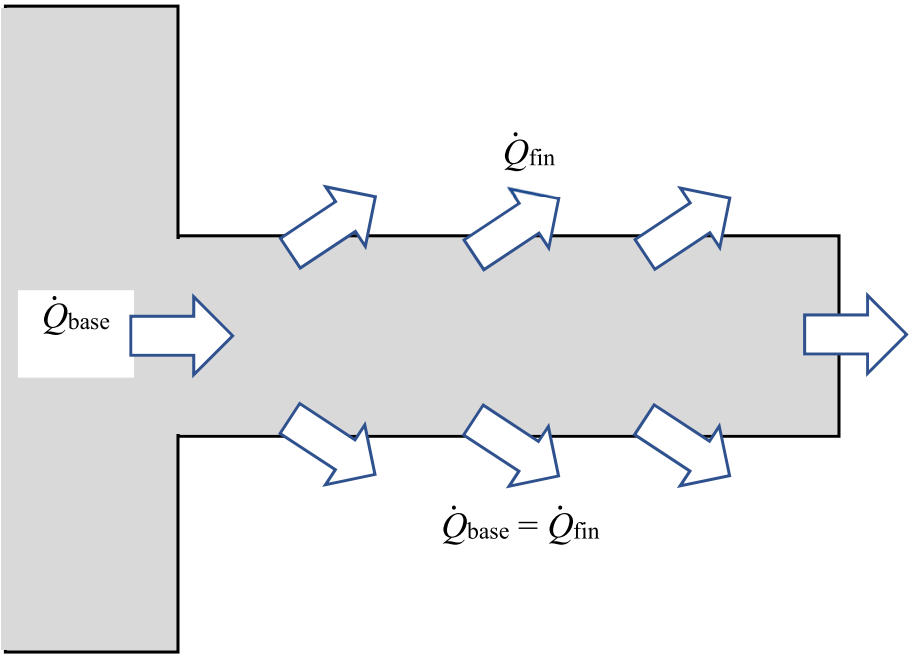

Fig. 10. Fin heat about transfer process.

silicon sprays must be applied to the weld itself. It was found from AS/NZS 3990–2016 [54] that the maximum permissible stress for a fillet weld is 140 MPa due to the design by Sharma et al. [35] being a larger scaled design it was found that the maximum amount of stress occurring in the system was 0.5 MPa. It can be said that welding is easily compliant with this design. It was identified in AS/NZS 2312.2–2014 [53] that distortion cracking can occur to galvanized steel during repeated heating and cooling environments, this occurs with large amounts of force occurring to a galvanized steel member. Fortunately, due to the small amount of stress experienced and the fact that the 10 mm fillet welds holding the frame together, this design will comply with the standard.

Secondly and *thirdly*, PCM tubes and fins were selected and made from aluminum and galvanized aluminum for the PCM end cap respectively. Due to the PCM tubes not occurring any stresses due to them simply sitting in the water tank unsupported, any forces compliance can be neglected. The only parameters that need to be compliant are the welding of the fins to the tubes as well as the heat treatment due to everyday testing. Consulting AS/NZS 1664.1–1997 [55] for aluminum structures it was found for welding alloys with a T1 temper with filler alloy that a minimum of 6 mm thick throat must be used. For this design, it has been specified that a 7 mm throat be used to ensure compliance. Consulting AS/NZS 1664.1–1997 [55] again regarding heating of aluminum it has been found that heating of any members beyond 200°*C* can only be done so for a maximum of 30 min. This design will encounter a maximum of 80°*C* and then be left to cool immediately, this shows that the design is compliant for heating purposes.

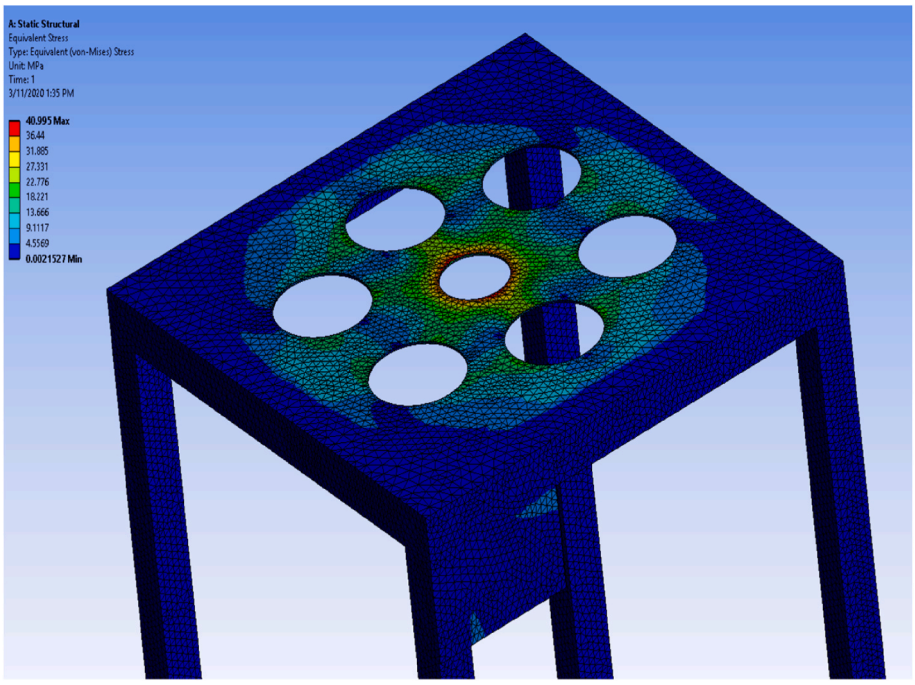

(a): Heater frame equivalent stress response

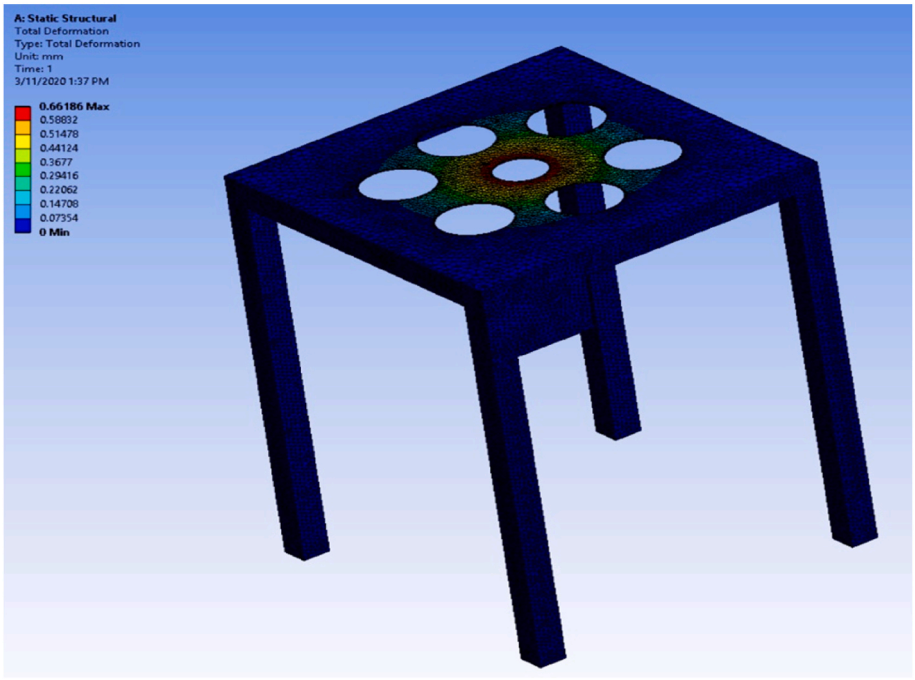

(b): Heater frame total deformation response

Fig. 11. (a): Heater frame equivalent stress response. (b): Heater frame total deformation response.

Fourthly, the Frame that was selected as hot-dipped, Zinc coated galvanized sheet metal for the top and hot-dipped galvanized (Duragal) SHS Steel. AS 3990–2016 [54] relates to the fatigue found in steelwork in mechanical equipment. This design is static but due to the tasks of operation with constantly moving PCM tubes as well as the heater fatigue can occur. It is found that in regions where high-stress concentrations in particular for this frame design being the heater hole that fatigue cracking can occur. Consulting standard fins efficiency curves [51] representing the equivalent stress FEA it is observed that a maximum of 40.9 MPa is occurring to this location (Fig. 11(a)), due to

this being the only force applied and with no additional force occurring over time, it can easily be stated that this design is safe and compliant. Consulting Table 2.1 from AS 4100–2020 [56] with a plate of 1.6 mm thickness a maximum of 250 MPa can be experienced before failure, due to the maximum stress experienced in this design being 40 MPa it can safely be said that this design is compliant. It was found in the previous section from AS 3990–2016 [54] that the maximum permissible stress for a fillet weld is 140 MPa once again observing the FEA models developed if can be safely said that this design can handle the relevant stresses exerted on the frame.

3.3. Assembly

The manufacturing component of this PCM testing apparatus [57] is quite simple in terms of complexity, once again the different components of the design will be broken up to identify the different manufacturing processes required. The water tank can be made by water jet cutting to relevant specifications, rolling the sheet metal to meet the required diameter, and then MIG weld the bottom and rolled tank part together. PCM tubes and Fins [58,59] are also be prepared by water jet cutting the rings for the annular fins and then TIG welding them onto the round tube. The PCM end cap was can be purchased off-the-shelf. The frame was selected to be made by drop saw cutting of the SHS steel, Water jet cutting of the sheet metal, and MIG welding of the components for assembly.

The assembly of this design was relatively simple as the setup for testing took minimal time. The frame was designed to sit over the top of the water tank as there was no exact positioning for this, however for testing it is recommended to sit the tank as centered as possible under the frame. The end caps for the tubes simply push onto the tubes, this will be a tight fit as no water or PCM should interact with one another. The tubes will slide through the relevant holes until it is at the bottom of the tank, due to the tubes sitting at the bottom of the tank the end cap will not fall off. The immersion heater simply sits through the middle hole in the frame and the thermostat can be fixed to the plate on the frame. Due to minimal knowledge being known about the thermostat the positioning method is unknown, however, it is assumed simple fixing will be completed by drilling screws into the plate attached to the frame. For conceptualization of the assembly of this design, the annotated drawings attached with this submission can be observed, however for simple understanding Fig. 12.

3.4. Predicted prototype performance and validation

The final design developed is similar to that completed by Sharma et al. [35] where a tank and PCM tubes were used. The first parameter that is improved is the introduction of a frame to support the PCM tubes. The previous design essentially had the tubes sitting freely in the tank. It was considered that these tubes could fall over during testing so incorporating a frame is useful. The frame also provided an access point for a heater so maneuverability for testing can occur, the design from Sharma et al. [35] did not take this component into account. The tank

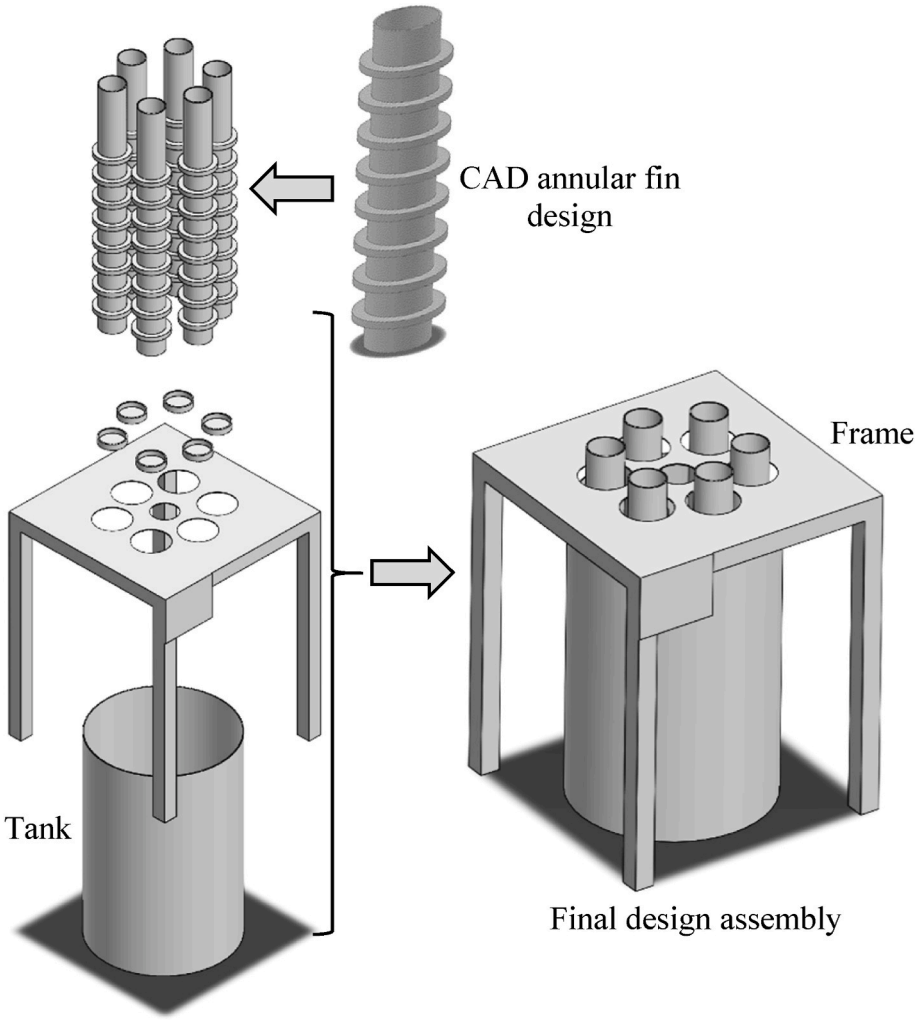

Fig. 12. Final design.

dimensions for the design by Sharma et al. [35] were designed with no critical dimensions, through further research the final design developed is backed by supported formula ensuring success. The implementation of fins is a new concept not seen in any literature surrounding this topic, through finding the critical dimensions and the influence through heat transfer, this new design will be superior to other investigations. The size of this new design is much smaller than that developed by Sharma et al. [35] as only 17.2 L of water will be tested rather than 250 L. This smaller scale was decided so testing would not take long to complete, as there are several PCM types and combinations that could be tested being able to quickly test variables and understand the response accurately is the intention behind this design. Overall, in this final design every decision made has been influenced by thermodynamic calculations so when testing occurs the results developed will be accurate.

4. Discussion

This study was to design an improvement of a testing apparatus to replicate the functions of a solar thermal water heating system. This testing apparatus had to be able to allow several PCM types, combinations and overall ratio amounts to be tested at high temperatures and allowed to cool. The design being proposed has much smaller than other designs seen in literature as it was decided to reduce the testing time allowing fast interchangeable tests to be completed in the future. The water tank holding the water, PCM tubes, and the PCM itself has considered with no insulation and exposed to the atmosphere to increase the time it would take to cool the apparatus. The water tank has assumed to be developed using 1.6 mm thick galvanized steel due to its simple manufacturing process of rolling the metal on a press. Completing natural convection calculations on the water tank it was found how long it will take to cool the tank without the influence of PCM. This can be used as a baseline for testing as the time is taken using different PCM parameters can be compared to this 15-min base time to understand how much influence they pose. Through completing supported calculations, a water tank design that will adequately hold the water has proposed and it can be assumed that through testing the results will be accurate.

Implementing annular fins to the PCM tubes is a technique not seen in the literature surrounding this research topic. Through completing the relevant heat transfer calculations, it has found that the heat transfer between the PCM tube and the water increased, ensuring that the thermal performance of testing will show a significant increase. Choosing the tubes and fins as aluminum is a strong design choice due to their lightweight and ability not to corrode from the PCMs. The frame that sits over the tank is a new design also not seen in literature, being able to hold the water heater as well as support the PCM tubes is a simplistic design choice. It has found that this frame will be lightweight (15 kg) and will be easily maneuverable as only one person can move it by hand. The heater can be simply placed through the hole with a good connection to the water in the tank, where the digital thermostat that can be mounted to the frame is useful due to its ability to accurately heat the water during testing. Through completing FEA it is found that this design can adequately handle the performance of the operation, due to the many cycles of testing it can be assured that this frame design can handle the requirements of testing.

Through consulting relevant Australian Standards, it has found that this design is compliant and will operate in a safe fashion. There are not many loads or forces that are applied to this testing apparatus so it can easily be stated that this design is suitable. From researching the materials and off-the-shelf components a total cost of approximately $1300.00 will be required to fully set up this apparatus. This design is functional due to its ability to reuse off-cuts from previous components making this design cost-effective. Due to the manufacturing mostly consisting of cutting to specifications and then welding, all manufacturing processes can be completed at common workshops.

5. Conclusions

The current energy crisis has deviated the attention of the whole world towards finding replacements for fossil fuels. Even with the presence of solar energy it was not much appreciated earlier because it could only be used if the source were available. It was found that thermal energy cannot be stored for long durations in hot water systems after dark due to the heat transfer of the stored energy to the surrounding atmosphere. Fortunately, due to research in this industry, it has been recently found that PCMs are being implemented into these storage systems to enhance the storage of solar energy. However, the concept of combining these PCMs types with different ratios is an area within this field that has not yet been investigated. This design research developed a testing apparatus that replicates a typical water heater used to test these PCM types and ratios to understand effectively how high this thermal enhancement is. This research used supported calculations, Computer-Aided modeling (CAD), and Finite Element Analysis (FEA) to proposed an improved design that will suitably test this design problem with ensured success. This proposed design is light, cost-effective, and complies with relevant Australian and New Zealand Standards so it can be confidently stated that this design developed is optimal for its intended use and at least 10% efficiency improvement.

Credit author statement

Greg Wheatley – Conceptualization, Methodology, Validation, Formal analysis, Investigation, Resources, Supervision, Project administration. Robiul Islam Rubel - Writing - Review & Editing, Validation, Formal analysis, Supervision, Project administration

Declaration of competing interest

The authors declare that they have no known competing financial interests or personal relationships that could have appeared to influence the work reported in this paper.

Acknowledgment

The authors gratefully acknowledge support from James Cook University, James Cook Dr, Douglas QLD 4814 Australia.

References

[1] D. Pimentel, X. Huang, A. Cordova, M. Pimentel, Impact of a growing population on natural resources: the challenge for environmental management, Front. Interdiscip. J. Study Abroad 3 (2) (1997), https://doi.org/10.36366/frontiers.v3i1.48.
[2] I. Sarbu, C. Sebarchievici, A comprehensive review of thermal energy storage, Sustainability 10 (1) (2018), https://doi.org/10.3390/su10010191.
[3] J.P. Holdren, Population and the energy problem, Popul. Environ. 12 (3) (1991) 231–255. https://www.jstor.org/stable/27503199.
[4] OECD Green Growth Studies, Energy, OECD iLibrary, 2012, https://doi.org/10.1787/22229523.
[5] F.S. Javadi, H.S.C. Metselaar, P. Ganesan, Performance improvement of solar thermal systems integrated with phase change materials (PCM), a review, Sol. Energy 206 (2020) 330–352, https://doi.org/10.1016/j.solener.2020.05.106.
[6] Australian Energy Resource Assessment, Chapter 10: solar energy, in: Geoscience Australia, 2013. https://arena.gov.au/assets/2013/08/Chapter-10-Solar-Energy.pdf.
[7] S.D. Sharma, K. Sagara, Latent heat storage materials and systems: a review, Int. J. Green Energy 2 (1) (2005) 1–56, https://doi.org/10.1081/GE-200051299.
[8] P.A. Owusu, S. Asumadu-Sarkodie, A review of renewable energy sources, sustainability issues and climate change mitigation, Cogent Eng 3 (1) (2016), https://doi.org/10.1080/23311916.2016.1167990.
[9] D. Ranjan, A. Bahriye, K.S. Rohit, S. Kuljeet, Application of artificial bee colony algorithm for inverse modelling of a solar collector, Inverse Probl. Sci. Eng. 25 (6) (2017) 887–908, https://doi.org/10.1080/17415977.2016.1209748.
[10] K. Abhishek, V. Sunirmit, D. Ranjan, Eigenfunctions and genetic algorithm based improved strategies for performance analysis and geometric optimization of a two-zone solar pond, Sol. Energy (211) (2020) 949–961, https://doi.org/10.1016/j.solener.2020.10.032.

[11] G. Rohtash, D. Ranjan, Experimental analysis of a novel solar pond driven thermoelectric energy system, ASME. J. Energy Resour. Technol. 142 (12) (2020) 121302, https://doi.org/10.1115/1.4047324.
[12] Solar Energy. Geosince Australia, [cited 2021 July 21]. Available from: https://www.ga.gov.au/scientific-topics/energy/resources/other-renewable-energy-resources/solar-energy.
[13] Albeck-Ripka L, Penn I. How coal-loving Australia became the leader in rooftop solar. The New York Times, [cited 2021 July 21]. Available from: https://www.japantimes.co.jp/news/2020/10/05/business/coal-australia-rooftop-solar-power/..
[14] Bureau of Meteorology, Australian Government, Average annual and monthly sunshine duration, IDCJCM0013, 2005. [cited 2021 July 21]. Available from: http://www.bom.gov.au/jsp/ncc/climate_averages/sunshine-hours/index.jsp.
[15] Australian Renewable Energy Agency, Solar power. [cited 2021 July 21]. Available from: https://arena.gov.au/renewable-energy/solar/.
[16] A. Castell, C. Solé, Design of latent heat storage systems using phase change materials (PCMs). Advances in Thermal Energy Storage Systems: Methods and Applications, Woodhead Publishing Limited, 2015, https://doi.org/10.1533/9781782420965.2.285.
[17] P.V. Australian, Institute. State performance. https://pv-map.apvi.org.au/live.
[18] K.N. Nwaigwe, P. Mutabilwa, E. Dintwa, An overview of solar power (PV systems) integration into electricity grids, Mater. Sci. Energy Technol. 2 (3) (2019) 629–633, https://doi.org/10.1016/j.mset.2019.07.002.
[19] A. Kumar, S. Shukla, Solar thermal energy storage, Roorkee, in: International Meeting on Energy Storage Devices, 2018, https://doi.org/10.1007/978-981-10-7206-2_8. India.
[20] V. Sunirmit, D. Ranjan, Effect of ground heat extraction on stability and thermal performance of solar ponds considering imperfect heat transfer, Sol. Energy 198 (2020) 596–604, https://doi.org/10.1016/j.solener.2020.01.085.
[21] V. Sunirmit, D. Ranjan, K. Abhishek, Transient thermal modelling and optimization of a solar collector-type pond considering an improved decay of radiative intensity, Int. J. Therm. Sci. 139 (2019) 440–449, https://doi.org/10.1016/j.ijthermalsci.2019.02.008.
[22] K. Abhishek, D. Ranjan, Effect of peripheral heat conduction in salt-gradient solar ponds, J. Energy Storage 33 (2021), https://doi.org/10.1016/j.est.2020.102084.
[23] M.S. Malik, et al., Design and fabrication of solar thermal energy storage system using potash alum as a pcm, Ener. 13 (23) (2020), https://doi.org/10.3390/en13236169.
[24] L. Zheng, W. Zhang, F. Liang, A review about phase change material cold storage system applied to solarpowered air-conditioning system, Adv. Mech. Eng. 9 (6) (2017) 1–20, https://doi.org/10.1177/1687814017705844.
[25] M. Harald, F.C. Luisa, Heat and Cold Storage with PCM - an up to Date Introduction into Basics and Applications, 2008. https://www.springer.com/gp/book/9783540685562.
[26] A. Bayomy, S. Davies, Z. Saghir, Domestic hot water storage tank utilizing phase change materials (PCMs): numerical approach, Energies 12 (11) (2019), https://doi.org/10.3390/en12112170.
[27] M. Mofijur, T.M.I. Mahlia, A.S. Silitonga, et al., Phase change materials (PCM) for solar energy usages and storage: an overview, Energies 12 (16) (2019) 1–20, https://doi.org/10.3390/en12163167.
[28] L. Esteves, A. Magalhães, V. Ferreira, C. Pinho, Test of two phase change materials for thermal energy storage: determination of the global heat transfer coefficient, Chem. Eng. 2 (1) (2018) 1–16, https://doi.org/10.3390/chemengineering2010010.
[29] K. Faraj, M. Khaled, J. Faraj, F. Hachem, C. Castelain, A review on phase change materials for thermal energy storage in buildings: heating and hybrid applications, J Energy Storage 33 (2021), https://doi.org/10.1016/j.est.2020.101913.
[30] G. Murali, K. Mayilsamy, An overview of PCM usage to enhance solar water heating system, Int. J. Chem. Tech. Res. 7 (4) (2015) 1802–1807.
[31] A.F. Mohammad, A.A. Ali, Phase change material for enhancing solar water heater, an experimental approach, Energy Convers. Manag. 71 (2013) 138–145, https://doi.org/10.1016/j.enconman.2013.03.034.
[32] P. Jacobo, L.M. José, C. Bárbara, L. José de, M.P. José, On the behavior of different PCMs in a hot water storage tank against thermal demands, Materials 9 (3) (2016) 213, https://doi.org/10.3390/ma9030213.
[33] D. Eleni, et al., Phase change materials in solar domestic hot water systems: a review, Int. J. Thermofluids 10 (2021) 100075, https://doi.org/10.1016/j.ijft.2021.100075.
[34] E. Vengadesan, R. Senthil, A review on recent development of thermal performance enhancement methods of flat plate solar water heater, Sol. Energy 206 (June) (2020) 935–961, https://doi.org/10.1016/j.solener.2020.06.059.
[35] A. Sharma, C. Chen, Solar water heating system with phase change materials, Int Rev Chem Eng (I RE CH E). 1 (4) (2009) 297–307. http://www.hristov.com/jordan/pdfs/Solar%20Water%20Heating%20System%20with%20Phase%20Change%20Materials.pdf.
[36] N.K. Bansal, D. Buddhi, An analytical study of a latent heat storage system in a cylinder, Energy Convers. Manag. 33 (4) (1992) 235–242, https://doi.org/10.1016/0196-8904(92)90113-B.
[37] H. Jouhara, A. Żabnieńska-Góra, N. Khordehgah, D. Ahmad, T. Lipinski, Latent thermal energy storage technologies and applications: a review, Int J Thermofluids (2020) 5–6, https://doi.org/10.1016/j.ijft.2020.100039.
[38] B. Cárdenas, N. León, High temperature latent heat thermal energy storage: phase change materials, design considerations and performance enhancement techniques, Renew. Sustain. Energy Rev. 27 (2013) 724–737, https://doi.org/10.1016/j.rser.2013.07.028.
[39] F. Abdalla, P. Tuohy, D. Evans, P. Blackwell, A review of integrated phase change materials for evacuated tube solar collector system, in: International Congress on Energy Research, Alanya, Turkey, 2018, pp. 379–390. https://strathprints.strath.ac.uk/66957/.
[40] S.A. Mohamed, et al., A review on current status and challenges of inorganic phase change materials for thermal energy storage systems, Renew. Sustain. Energy Rev. 70 (2017) 1072–1089.
[41] G.K. Ijemaru, M.Z. Adamu, E.A. Obatoke, H. Hussaini, F.O. Ajayi, Design and modelling of a solar water heating system, Ind. Eng. Lett. 4 (12) (2014) 70–79. http://www.iiste.org/Journals/index.php/IEL/article/view/18842/19205.
[42] E. Nshimyumuremyi, W. Junqi, Thermal efficiency and cost analysis of solar water heater made in Rwanda, Energy Explor. Exploit. 37 (3) (2019) 1147–1161, https://doi.org/10.1177/0144598718815240.
[43] Bunea M, Eicher S, Hildbrand C, Bony J, Perers B, Citherlet S. Performance of solar collectors under low temperature conditions: Measurements and simulations results. In: Eurosun 2012, Rijeka Croatia 2012. https://task44.iea-shc.org/Data/Sites/1/publications/2012.025.pdf.
[44] Hudon K, Merrigan T, Burch J, Maguire J. Low-cost solar water heating research and development roadmap, United States. doi: https://dx.doi.org/10.2172/1050127.
[45] C. Rockenbaugh, J. Dean, D. Lovullo, et al., High Performance Flat Plate Solar Thermal Collector Evaluation, NREL, 2016. https://www.nrel.gov/docs/fy16osti/66215.pdf.
[46] Materials Used for Manufacturing Solar Domestic Hot Water Systems & Comments on Their Reliability, Energy Program, European Commission, 2004. http://exergia.gr/wp-content/uploads/materials-domestic-water.pdf.
[47] E. Skiba, Understanding Solar Collector Efficiency, 2011. http://www.apricus.com/upload/userfiles/downloads/Apricus-article-understanding-solar-collector-efficiency.pdf.
[48] P.M. Kumar, K. Mylsamy, Experimental investigation of solar water heater integrated with a nanocomposite phase change material: energetic and exergetic approach, J. Therm. Anal. Calorim. 136 (1) (2019) 121–132, https://doi.org/10.1007/s10973-018-7937-9.
[49] T. Li, Y. Liu, D. Wang, K. Shang, J. Liu, Optimization analysis on storage tank volume in solar heating system, Procedia Eng 121 (2015) 1356–1364, https://doi.org/10.1016/j.proeng.2015.09.019.
[50] N.S. Bondareva, M.A. Sheremet, Natural convection melting influence on the thermal resistance of a brick partially filled with phase change, Material. Fluids 6 (2021) 258, https://doi.org/10.3390/fluids6070258, 2021.
[51] Y. Cengel, A. Ghajar, Heat and Mass Transfer : Fundamentals and Applications, fifth ed., McGraw Hill, 2015. https://www.academia.edu/40468658/Cengel_heat_and_mass_transfer_5ed_rev.
[52] SCINTEX Immersion Heater. [cited 2021 July 21]. Available from: https://www.scintex.com.au/products/hose-tail-hose-nipple?variant=864366839&utm_source=fomo&utm_medium=notification.
[53] Standards catalogue AS/NZS 2312.2:2014, Australian Standard, [cited 2021 July 21]. Available from: https://www.standards.org.au/standards-catalogue/sa-snz/other/mt-014/as-slash-nzs–2312-dot-2-colon-2014.
[54] Standards catalogue AS 3990-1993 rec : 2016, Australian Standard, [cited 2021 July 21]. Available from: https://www.standards.org.au/standards-catalogue/sa-snz/building/me-005/as–3990-1993–rec-colon-2016.
[55] Standards catalogue AS/NZS 1664 . 1-1997, Australian Standards, [cited 2021 July 21]. Available from: https://www.standards.org.au/standards-catalogue/sa-snz/other/bd-050/as-slash-nzs–1664-dot-1-1997.
[56] Standards catalogue AS 4100 : 2020, Australian Standard, [cited 2021 July 21]. Available from: https://www.standards.org.au/standards-catalogue/sa-snz/other/bd-001/as–4100-colon-2020.
[57] Richard Opoku, John P. Kizito, Experimental investigation of heat transfer characteristics and performance of smooth and wicking surfaces in spray cooling for high heat flux applications, Results in Engineering 6 (2020) 100119, https://doi.org/10.1016/j.rineng.2020.100119. ISSN 2590-1230.
[58] You Lyu, Abu Raihan Mohammad Siddique, S. Andrew Gadsden, Shohel Mahmud.
[59] Experimental investigation of thermoelectric cooling for a new battery pack design in a copper holder, Results in Engineering 10 (2021) 100214, https://doi.org/10.1016/j.rineng.2021.100214. ISSN 2590-1230.

Nomenclature

Q: = Latent heat storage capacity (kJ/Kg)
T_i: = Initial fluid temperatures (K)
T_m: = Fluid melting temperatures (K)
T_f: = Fluid temperatures at an instant (K)
m: = PCM material mass (kg)
a_m: = Fraction of PCM material melt
Δh_m: = PCM latent heat of fusion (kJ/Kg)
C_{sp}: = PCM material specific heat capacity in solid state (kJ/Kg.K)
C_{lp}: = PCM material specific heat capacity in liquid state (kJ/Kg.K)
R_f: = Radiant flux striking the solar plate collector (W/m^2)
T_{cov}: = Transmittance of transparent cover of solar plate collector
A_p: = Exposed solar collector plate area (m^2)
G: = Irradiance of the solar plate collector (W/m^2)
$\propto_p$: = Absorbance of the solar plate collector
R_1: = Resistance to heat loss from the solar collector plate to surroundings (K/W)
T_p: = Temperature of the solar collector plate (K)
T_a: = Temperature of the surrounding area of solar collecotr plate (K)
P_u: = Useful power output from solar collector plate (W)

$\exists_c$: = captured efficiency of the solar collector plate
I: = Radiation intensity on the solar collector plate (W/m^2)
ΔT: = Temperature difference between solar collector plate and surrounding (K)
$\dot{m}$: = Mass flow rate of water in solar collecotr (kg/s)
η_c: = Solar thermal efficiency of the solar plate collector (%)
C: = Specific heat capacity of water (kJ/kgK)
T_1: = Inlet temperature for the mass in solar collector plate (K)
T_2: = Outlet temperatute for the mass in solar collector plate (K)
V: = Volume of water tank (m^3)
D_{out}: = Outer diameter of the PCM tube (m)
l: = Length of the PCM cylinder (m)
ε: = Water fraction
n: = Number of PCM tubes
r_{tank}: = Ideal radius of tank (m)
D_{tank}: = Ideal diameter of tank (m)
V_{water}: = Total volume of water in the solar collector (m^3)
V_{tank}: = Total volume of tank (m^3)
V_{tube}: = Total volume of PCM tubes (m^3)
h: = Convection heat transfer coefficient (W/m^{2}K)
T_f: = Film temperature (K)
T_{max}: = Maximum temperature of water (K)
T_{min}: = Minimum temperature of water (K)
Ra: = Rayleigh's number
g: = acceleration due to gravity (m/s^2)
β: = Thermal expansion coefficient (1/K)
v: = Kinematic viscosity (m^2/s)
T_s: = Tube surface temperature (K)
T_∞: = Fluid temperature far from the surface of the object (K)
Pr: = Prandtl number
Gr: = Grashof number
Nu: = Nusselt number
t: = time (s)
ρ: = density of water (kg/m^3)
C_p: = Specific heat capacity of water (kJ/Kg.K)
r: = Radius of tank (m)
T_0: = Temperature at time $t = 0$ (K)
T: = Temperature at time t (K)
η_{fin}: = Fin efficiency (%)
t_h: = Thickness (m)
L_C: = Critical length of fin (m)
Q_{fin}: = Heat transfer by fins (W)
$h_{no\ fins}$: = Convection heat transfer coefficient at no fins ((W/m^{2}K)
$A_{no\ fins}$: = Area of no fins for heat transfer (m^2)
$Q_{Single\ tube,\ no\ fins}$: = Heat transfer for single tubes with no fins (W)
$Q_{Total,\ no\ fins}$: = Total heat transfer for single tubes with no fins (W)
h_{finned}: = Convection heat transfer coefficient with fins (W/m^{2}K)
A_{finned}: = Area of fins for heat transfer (m^2)
$Q_{Single\ tube,\ finned}$: = Heat transfer for single tubes with fins (W)
$Q_{Total,\ finned}$: = Total heat transfer for single tubes with fins (W)